Change Detection Techniques for Monitoring Forest Clearing and Regrowth in a Tropical Moist Forest

Daniel J. Hayes

Dr. Steven A. Sader

Abstract

The once remote and inaccessible forests of Guatemala's Maya Biosphere Reserve (MBR) have recently experienced high rates of deforestation corresponding to human migration and expansion of the agricultural frontier. Given the importance of land cover and land use change data in conservation planning, accurate and efficient techniques to detect forest change from multi-temporal satellite imagery were desired for implementation by local conservation organizations. Three dates of Landsat Thematic Mapper, each acquired two years apart, were radiometrically normalized and pre-processed to remove clouds, water, and wetlands, prior to employing the change detection algorithm. Three change detection methods were evaluated: normalized difference vegetation index (NDVI) image differencing, principal component analysis, and RGB-NDVI change detection. A technique to generate reference points, by visual interpretation of color composite Landsat images, for Kappa-optimizing thresholding and accuracy assessment, was employed. The highest overall accuracy was achieved with the RGB-NDVI method (85%). This method was also preferred for its simplicity in design and ease in interpretation, which were important considerations for transferring remote sensing technology to local and international non-governmental organizations.

Introduction

With rapid changes in land cover occurring over large areas, remote sensing technology is an essential tool in monitoring tropical forest conditions. The remote and inaccessible nature of many tropical forest regions limits the feasibility of ground-based inventory and monitoring methods for extensive land areas. Initiatives to monitor land cover and land use change are increasingly reliant on information derived from remotely sensed data. Such information provides the data link to other techniques designed to understand the human processes behind deforestation (Lambin, 1994; Rindfuss and Stern, 1998).

An array of techniques are available to detect land cover changes from multi-temporal remote sensing data sets (Jensen, 1996; Coppin and Bauer, 1996). The goal of change detection is to discern those areas on digital images that depict change features of interest (e.g. forest clearing or land cover / land use change) between two or more image dates. One method, image differencing, is simply the subtraction of the pixel digital values of an image recorded at one date from the corresponding pixel values of the second date. The histogram of the resulting image depicts a range of pixel values from negative to positive numbers, where those clustered around zero represent no change and those at either tail represent reflectance changes from one image date to the next (Jensen, 1996). This method has been documented widely in change detection research (Singh, 1986; Muchoney and Haack, 1994; Green *et al.*, 1994; Coppin and Bauer, 1996; Macleod and Congalton, 1998). Some investigators favor this method for its accuracy, simplicity in computation, and ease in interpretation.

One difficulty encountered in employing image differencing for change detection is the selection of the appropriate threshold values in the histogram that separates real and spurious change. The subjectivity of threshold placement may be improved by the analyst's familiarity with the study area as well as access to ancillary data such as field information, GIS data, and/or matching dates of aerial photography. Fung and LeDrew (1988) tested quantitative methods for developing these threshold levels using accuracy indices. They recommended the Kappa coefficient of agreement in determining an optimal threshold level, being based on an error matrix of image data against known reference data.

Image differencing, although mathematically simple, allows for only one band of information to be processed at a time. Other techniques incorporate multiple bands of data for change detection. Several studies have demonstrated the utility of the principal component analysis (PCA) technique in multi-temporal image analysis (Byrne *et al.*, 1980; Fung and LeDrew, 1988; Muchoney and Haack, 1994; Coppin and Bauer, 1996; Macleod and Congalton, 1998). The results of using the PCA transform on two dates of imagery are contrary to that of its typical, one-date transformations. In multi-temporal analysis, the first two components tend to represent variation associated with unchanged land cover and overall image noise (i.e. atmospheric and seasonal variation), while the third and later components are of more interest in identifying change areas (Byrne *et al.*, 1980). Previous studies have confirmed that the minor components have been successful in detecting land cover changes (Byrne *et al.*, 1980; Fung and LeDrew, 1987) when the areas affected by change of interest occupy a small proportion of the study area (Fung and LeDrew, 1987; Macleod and Congalton, 1998).

Image differencing using band ratios or vegetation indices is another technique commonly employed for land cover change detection. For example, the normalized difference vegetation index (NDVI) was developed for use in identifying health and vigor in vegetation, as well as estimates of green biomass. The NDVI, the normalized difference of brightness values from the near infrared and visible red bands, has been found to be highly correlated with crown closure, leaf area index, and other vegetation parameters (Tucker, 1979; Sellers, 1985; Singh, 1986; Running *et al.*, 1986). Lyon *et al.* (1998) compared seven vegetation indices to detect land cover change in a Chiapas, Mexico study site.

They reported that the NDVI was least affected by topographic factors and was the only index that showed histograms with normal distributions. Change in canopy cover or vegetation biomass can be detected by analyzing NDVI values from separate dates (e.g. NDVI image differencing).

Sader and Winne (1992) developed a technique to visualize change using three dates of NDVI imagery concurrently and interpretation concepts of color additive theory. By simultaneously projecting each date of NDVI through the red, green, and blue (RGB) computer display write functions, major changes in NDVI (and hence green biomass) between dates will appear in combinations of the primary (RGB) or complimentary (yellow, magenta, cyan) colors. Knowing which date of NDVI is coupled with each display color, the analyst can visually interpret the magnitude and direction of biomass changes in the study area over the three dates. Automated classification can be performed on three or more dates of NDVI by unsupervised cluster analysis (Sader *et al*., In Press). Change and no change categories are labeled and dated by interpreter analysis of the cluster statistical data and guided by visual interpretation of RGB-NDVI color composites.

Study Area and Background

Spanning approximately 2 million hectares of northern Guatemala, the Maya Biosphere Reserve (MBR) is an area of lowland tropical forests and expansive freshwater wetlands, part of the largest contiguous tropical moist forest remaining in Central America (Nations *et al*., 1998). The MBR is a complex of delineated management units including five national parks, four biological reserves (*biotopos*), a multiple use zone, and a buffer zone (Figure 1). The once remote and inaccessible forests of the region have experienced high rates of deforestation in the last decade, corresponding to human migration and expansion of the agricultural frontier (Sader *et al*., 1997).

Sader and colleagues (Sader *et al*., 1997; and Sader *et al*., In Press) have monitored rates and trends of forest clearing using Landsat Thematic Mapper (TM) imagery from the mid-1980's to late 1990's. Guatemalan government agencies and non-governmental organizations (NGOs) rely on regularly updated maps of the MBR to monitor deforestation patterns and disturbance in sensitive areas of the reserve. International donor agencies require the NGOs to quantify forest clearing rates at two-year intervals. Accurate and efficient techniques for extracting quantitative forest change data from remotely sensed images are needed to support the MBR forest monitoring program. Furthermore, this data is needed for analysis with community level socio-economic survey data concerning the driving forces of environmental change in the MBR (Schwartz, 1998; Hayes, 1999).

This paper describes the techniques used to process and validate multi-temporal Landsat TM imagery (3 dates) for obtaining time-series forest clearing and regrowth data in the MBR. Three change detection methods are compared: NDVI image differencing, PCA change detection, and RGB-NDVI classification. A visual interpretation technique to generate reference points from color composite Landsat images, for selecting Kappa-optimizing thresholds and for assessment of classification accuracy, is described. The goal is to determine the most accurate and efficient method to detect forest change in the MBR's tropical moist forest and to facilitate the transfer of this technology to the local NGOs.
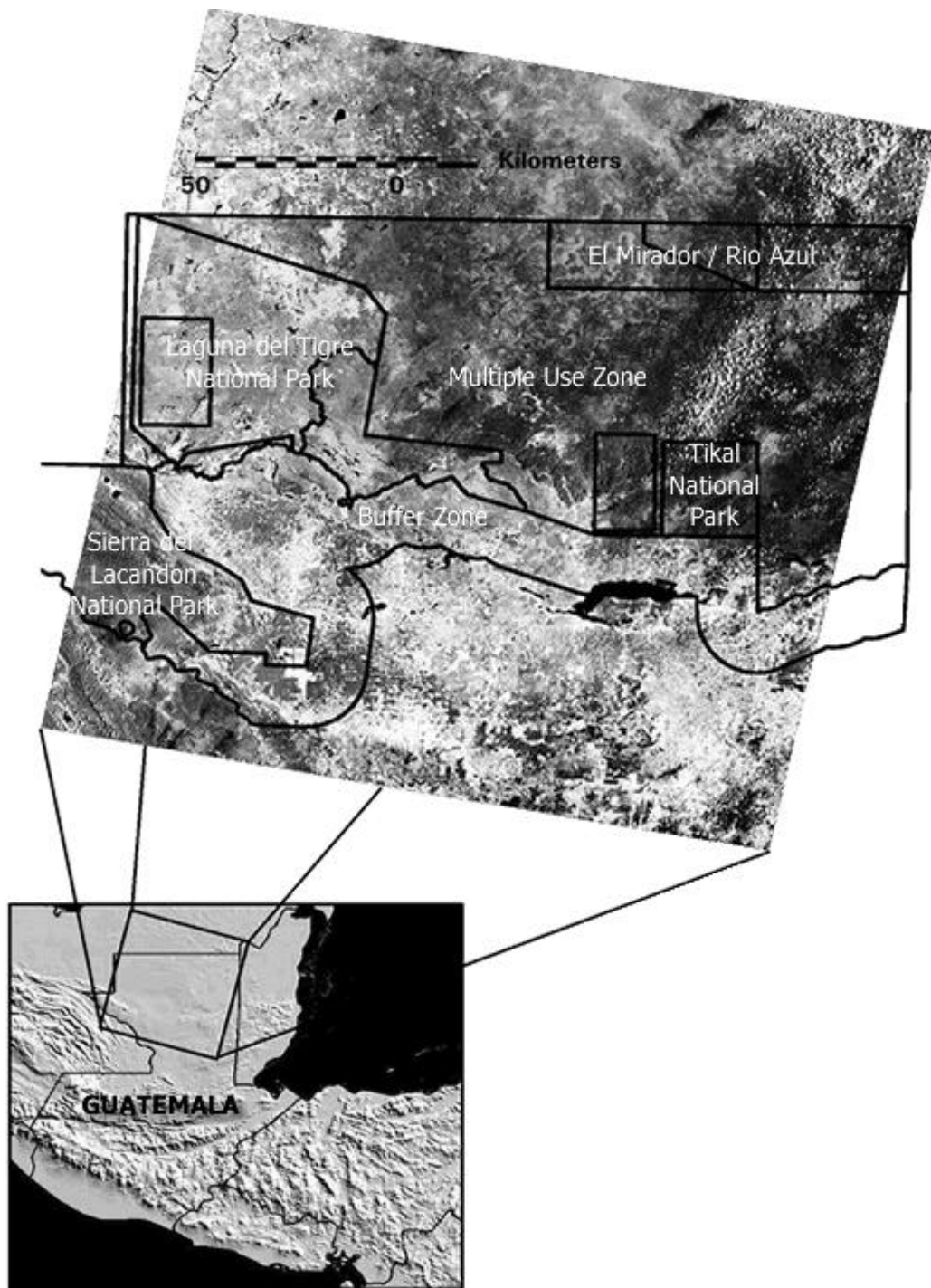
Figure 1

Methods

Data Acquisition and Pre-processing

Three dates of Landsat TM imagery (1993, 95, 97) for WorldWide Reference System path 20, row 48 were acquired. This Landsat scene comprises approximately 90% of the MBR and buffer zone (Figure 1). To reduce scene-to-scene variation due to sun angle, soil moisture, atmospheric condition, and vegetation phenology differences, all data were collected between the months of March and May,

corresponding to the MBR's dry season. Each scene was georeferenced to a previously rectified 1995 TM image. TM bands 3 (visible red), 4 (near infrared), and 5 (mid-infrared) were extracted from the original TM data sets to reduce between-band correlation, data volume, and processing time. Previous studies have shown that selecting one band each from the visible, near infrared, and mid-infrared spectral regions results in the optimal waveband combination for vegetation discrimination (DeGloria, 1984; Horler and Ahern, 1986; Sader, 1989). Bands 3, 4, and 5 were input into "isodata" (ERDAS, 1997), an unsupervised classification module, to produce 200 spectral clusters. Binary images were created to isolate water, clouds, and cloud shadows through a combination of analyst definition of cloud/water clusters and on-screen editing. A previously developed image of non-forested wetlands and natural savannas was also added to the cloud and water image. These classes, being of no interest to forest clearing and regrowth analysis, were masked for all dates of imagery to avoid confusion in the change detection classification.

Radiometric Normalization

A relative radiometric calibration technique was applied to each band from each date of imagery. The technique incorporated linear regression methods reported by Eckhardt *et al*. (1990), Hall *et al*. (1991), and Jensen *et al*. (1995). The 1997 TM scene, which was corrected for sensor gain and bias, was used as the reference image to which the 1993 and 1995 data were normalized. First, normalization targets were selected from the wet (e.g. deep, clear water) and dry (e.g. urban features) non-vegetated extremes of each band (TM 3, 4, and 5) at each date (1993, 95, 97) by visual interpretation of the imagery and querying the digital numbers of pixels representing these features. The selection criteria were based on procedures outlined by Eckhardt *et al*. (1990). Each target consisted of an analyst-defined area of interest (AOI), which included the greatest number of pixels covering the target, whose digital numbers (DNs) were located at the extremes of the image histogram and collectively contained low variance.

The mean value of the pixel DNs was generated for each of the normalization target AOIs (each band, each date). The parameters used in the linear regression equation were calculated by the following "rectification transform" (from Hall *et al*., 1991):

$$m = \frac{Br - Dr}{Bs - Ds} \quad \text{and} \quad b = \frac{DrBs - DsBr}{Bs - Ds} \qquad \text{(Eq. 1)},$$

where: Br = the mean DN for the bright target of the reference image;
  Bs = the mean DN for the bright target of the subject image;
  Dr = the mean DN for the dark target of the reference image; and
  Ds = the mean DN for the dark target of the subject image.

Using linear regression, the corrected pixel values for the subject image (Y) were calculated from the original DN (X), for each band (i), by the following equation:

$$Y_i = m_i X_i + b_i \qquad \text{(Eq. 2)}.$$

Change Detection Methods

Three change detection methods (NDVI differencing, PCA, RGB-NDVI classification) were independently applied to the cloud / water masked and radiometrically normalized time-series TM data set. A three-date forest change detection classification of the selected study area was generated from each method. Each method was evaluated and compared with the other methods on its ability to classify temporal states in forest cover (i.e. cleared, regrown, no change) over the three time periods. The methods were evaluated and contrasted on the basis of classification accuracy (Congalton, 1991), efficiency in computation and processing, and ease in interpretation.

NDVI image differencing

Difference images were created by first calculating NDVI values for each date (j) of imagery by the following equation:

$$NDVI[j] = \frac{(TM4 - TM3)}{(TM4 + TM3)} \qquad \text{(Eq. 3).}$$

Two difference images were created by subtracting one date of NDVI values from those of the previous date, so that:

$$DIF[9395] = NDVI[95] - NDVI[93] \;\text{ and }\; DIF[9597] = NDVI[97] - NDVI[95] \qquad \text{(Eq. 4).}$$

Principal component analysis

The principal component transformation was performed separately on two data sets (1993 and 1995, 1995 and 1997) using three TM bands (3, 4, and 5) for each date. Each two-date data set contained six bands. The transformation used the "prince" routine (ERDAS 1997), modified to calculate the transform from a correlation matrix of the data set. Several authors have compared this "standardized" approach to PCA against transformations based on the covariance matrix (Conese *et al*., 1988; Eastman and Falk, 1993; Rencher 1995). Reported advantages of the standardized approach include improved interpretability, the isolation of seasonal effects and variability due to noise, better statistical control, and more precise classification. For each data set, the "standardized" PCA routine output included six component images, a table of eigenvalues quantifying the proportion of variance explained by each component, and a matrix of eigenvectors (weights or factor loadings) depicting between-date correlation for each band with each component. Components that represent change typically show an absence of correlation among bands between dates (Byrne *et al*., 1980). The component that best highlights the change of interest is chosen for thresholding, using visual interpretation of component images and analysis of the eigenvector matrix.

Image interpretation was based on the assessment of spatial continuity, by seeking out the components that express the differences in the changes of interest as spatially discontinuous areas within the image. The eigenvector analysis examined the algebraic signs on the weights. Differences between dates are expressed by the weight of one band at one date having an opposite sign as the same band of the other date. Based on these criteria, two of the six components (components 3 and 4 for each 2-date data set) were selected from the PCA for thresholding of no change and change areas. Of these two components, the one that showed the highest ability to threshold forest clearing / no change / regrowth (i.e. the highest estimated Kappa according to the reference sample points) was chosen for final classification.

RGB-NDVI classification

NDVI values from three dates (as calculated by Eq. 3) were classified into 50 spectral clusters. For each cluster class, the mean NDVI values at each date (1993, 1995, 1997) were categorized as very high, high, medium-high, medium, medium-low, low, or very low, based on the distribution of NDVI values over the study area. These levels of NDVI were established on the observation that, as most of the study area is composed of undisturbed forest, values within ±0.5 standard deviations from the mean represented high green biomass (high mean NDVI). The other NDVI levels were set at intervals of 0.5 standard deviations outward from the mean. Each cluster was examined for changes in NDVI levels over time. Clusters were named according to type of change (clearing, regrowth, or no change) and the corresponding time period(s) of change according to the NDVI levels as they related to three-date RGB-NDVI interpretation (Plate 1).
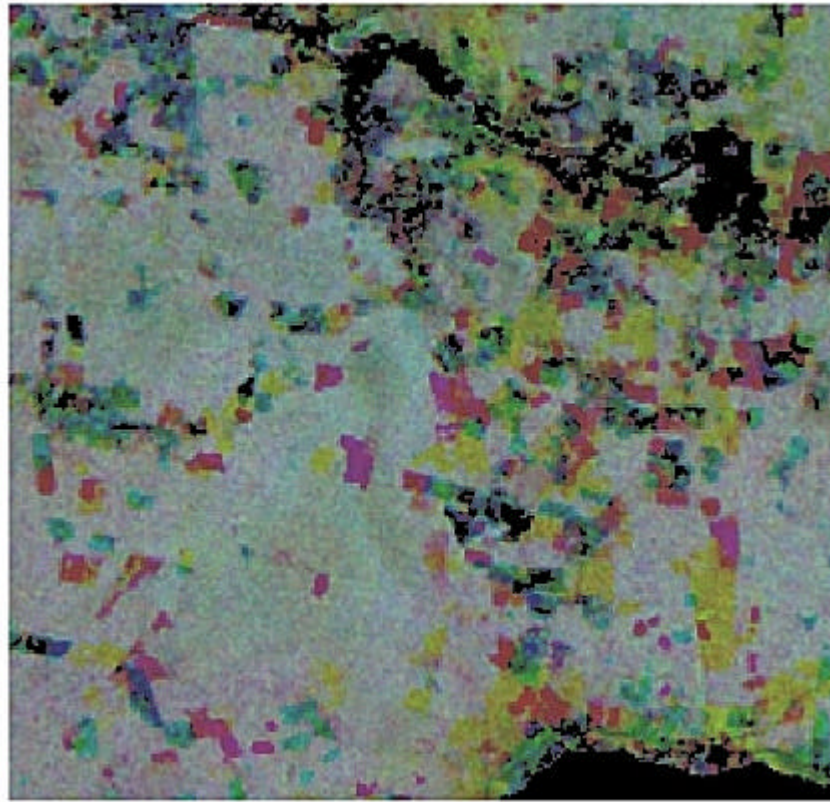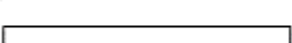
Computer Display Image Color	RED 1993 NDVI	GREEN 1995 NDVI	BLUE 1997 NDVI	Interpretation relative to Forest canopy changes
(blue)	low	low	high	Cleared before 93, regrow 95-97
(cyan)	low	high	high	Cleared before 93, regrow 93-97
(green)	low	high	low	Cleared before 93, regrow 93-95, cleared 95-97
(red)	high	low	low	Cleared before 93-95, regrow 95-97
(magenta)	high	low	high	Cleared before 93-95, regrow 95-97
(yellow)	high	high	low	Cleared before 95-97
(white)	high	high	high	No change, high NDVI forest
(black)	low	low	low	No change, low NDVI urban, pasture, other

Plate 1

Classifying the Change Images

Both the NDVI differencing and the PCA methods result in images with an 8-bit (0-255) data range. Thresholds must be identified along the histograms to separate change (both clearing and regrowth) from no change. Threshold levels were set quantitatively according to the optimal estimated Kappa coefficient, based on an error matrix of image data against known reference data (Fung and LeDrew, 1988).

Cohen *et al*. (1998) selected a random sample of points from a classified image and displayed them on each date of raw TM, RGB color composite imagery. Each point was then labeled as change (clearcut harvest) or no change by visual interpretation of the images, and used as the reference for accuracy assessment. They found the resulting error matrix to be not significantly different than one prepared with an independent vector database derived from aerial photography interpretation and ground truth methods.

For each change image, an error matrix was developed using a sample of visually interpreted points as reference against the values of the change image. To assure an adequate distribution of sample points to each change class, each 8-bit (0-255) change image was recoded into 32 classes with each class corresponding to 8 original digital values (0-7, 8-15, …, 248-255). This 32-class temporary file was then used to generate a stratified random sample of points to be interpreted for use as reference in the thresholding procedure. A 3x3 moving window was used to select sample points in which all the surrounding pixels were of the same class (9 out of 9 majority), thus avoiding edge effects in interpretation. Five sample points were generated from each of the 32 classes in the temporary file (n=160).

In the absence of existing historical reference data for the study area, the visual interpretation method reported by Cohen *et al*. (1998) was the only option for developing reference data for error matrices. Prior to visual satellite image interpretation, examples of newly cleared forest and recent forest regrowth were located on aerial photos and video frames available for a portion of the MBR study area in 1997. These sites were then examined on the 1993, 95, and 97 TM color composites (RGB 453) in order to train or "calibrate" the interpreter to the visual appearance of forest clearing and regrowth sites on the satellite imagery (Plate 2).

1993 Landsat TM 453

1995 Landsat TM 453

1997 Landsat TM 453

1997 True Color Photo Mosaic
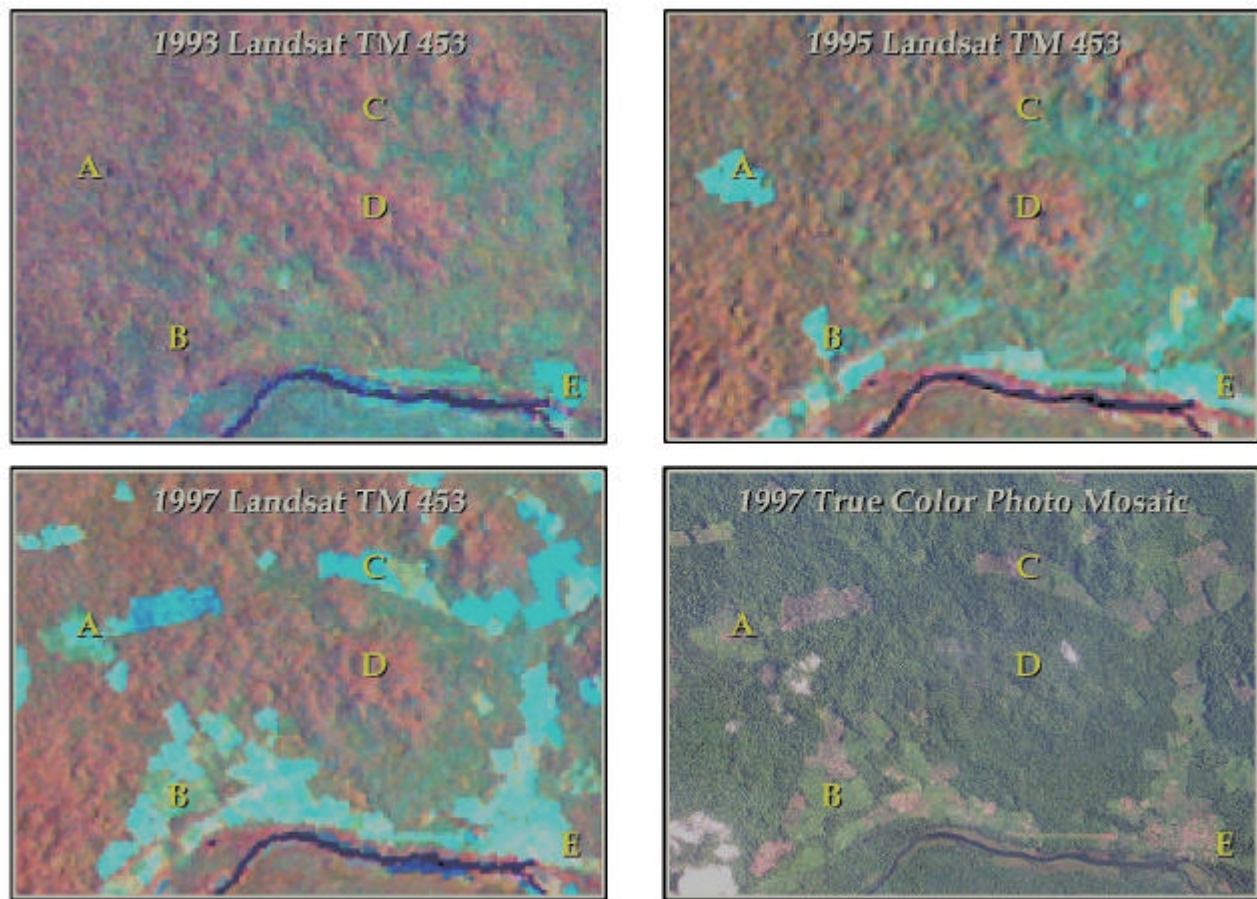
Plate 2

Table 1.

Cleared Vs. Not Cleared

Reference Data

Classified Data	Cleared	Not cleared	Row Total
Cleared	41	6	**47**
Not cleared	8	105	**113**
Column Total	**49**	**111**	**160**

Overall Accuracy = 91.3%   **KHAT** = 0.79

Not regrown vs. Regrown

Reference Data

Classified Data	Not regrown	Regrown	Row Total
Not regrown	127	6	133
Regrown	4	23	27
Column Total	131	29	160

Overall Accuracy = 93.8%   **KHAT** = 0.78

Overall agreement

Reference Data

Classified Data	Cleared	No change	Regrown	Row Total
Cleared	41	6	0	47
No change	8	72	6	86
Regrown	0	4	23	27
Column Total	49	82	29	160

Overall Accuracy = 85.0%   **KHAT** = 0.75

The three-date RGB-NDVI method used an unsupervised clustering routine rather than a thresholding technique to classify forest clearing, regrowth, and no change areas between image dates. However, the reference data developed for thresholding the change images was used to help name the spectral clusters. A matrix was developed to show agreement between the named RGB-NDVI clusters and visually interpreted sample points. Clusters that represented change, or showed confusion between known change and no change, were subset from the total cluster set. The remaining clusters (about half of the original 50) represented more subtle variation in NDVI levels of the forest canopy, not changes resulting from clearing or regrowth. These clusters were classified as "no change" while change and confusion clusters were reclassified from the original NDVI data into 50 new clusters. Jensen (1996) referred to this technique as "cluster busting". By separating no change forest from the clusters of significant change, it was expected that the discrimination of forest change and dates of occurrence would be improved. This was indeed the case, as the 50 new clusters were again compared with reference data and showed less confusion between clearing, regrowth, and no change classes. Using the cluster signature statistics and additive color theory interpretation of the raw RGB-NDVI image (Plate 1), these new clusters were categorized according to the type and time period of change. This image was then recombined with the no-change forest class from the first iteration to produce the final RGB-NDVI change detection classification.

Accuracy Assessment

Error matrices were developed to evaluate the ability of each method to discriminate between forest clearing, vegetation regrowth, and no change, for each time period of the analysis. Because the time-series analysis covered three dates, each two-date change detection classification from the NDVI differencing and PCA methods were combined into a three-date change detection classification covering 1993, 95, and 97 (Table 2). The RGB-NDVI produced a three-date change image directly through unsupervised classification.

TABLE 2.

1	**Cleared before 1993, regrowth 1995-97**
2	**Cleared before 1993, regrowth 1993-97**
3	**Cleared before 1993, regrowth 1993-95, cleared 1995-97**
4	**Cleared 1993-95, no regrowth**
5	**Cleared 1993-95, regrowth 1995-97**
6	**Cleared 1995-97**
7	No change

The results of the change detection methods were evaluated against a stratified random sample of reference points, using an error matrix constructed for each method. Visual interpretation of each date of color composite imagery, for each sample, was used to create the reference data (Plate 2). The seven change detection classes (Table2) were used to stratify the sample points. Selected sample points were limited to cases in which all pixels in a 3 x 3 window were of the same class (9 out of 9 majority). This was done to simplify visual interpretation and avoid edge effects. Ten samples were selected from each change class for a sample size of 70 from each image. The sample points from the three images were pooled (3 x 70) for a total sample of 210 points. This sample was independent of the one used for thresholding the NDVI difference and PCA change images and naming the three-date RGB-NDVI unsupervised clusters.

Producer's and user's accuracy were calculated for each change class, along with the overall accuracy, estimated Kappa, and Z-statistic for each classification. The error matrices of the three methods were compared for statistical differences by pair-wise comparison of the Z-statistics (Congalton and Green, 1999).

Results

The correlation and eigenvector matrices are shown in Tables 3a (for the 1993 to 1995 change image) and 3b (for the 1995 to 1997 change image). For both 2-date change transformations, the first component contained over 50% of the variation among the 6 bands (54.10% for 95-97 and 53.21% for 93-95). The first two components represented 79.15% of the variation in the 95-97 data set, and 76.02% of the variation in the 93-95 set. Visual analysis of the images corresponding to these components suggested that this variation could be attributed to atmospheric, seasonal, and other differences evenly distributed over all pixels.

TABLE 3A.

PCA [9395] Correlation Matrix

Bands	93tm3	93tm4	93tm5	95tm3	95tm4	95tm5
93tm3	1.0000	-0.4920	0.7225	0.6708	-0.1713	0.5637
93tm4	-0.4920	1.0000	-0.2090	-0.2860	0.4058	-0.1106
93tm5	0.7225	-0.2090	1.0000	0.5695	0.0180	0.7243
95tm3	0.6708	-0.2860	0.5695	1.0000	-0.2938	0.7648
95tm4	-0.1713	0.4058	0.0180	-0.2938	1.0000	0.0284
95tm5	0.5637	-0.1106	0.7243	0.7648	0.0284	1.0000

PCA [9395] Eigenvector Matrix (from Correlation Matrix)

	Component					
Bands	**1**	**2**	**3**	**4**	**5**	**6**
93tm3	0.4919	-0.0526	0.3171	-0.2605	0.6394	0.4219
93tm4	-0.2679	0.5779	-0.5726	-0.4009	0.3100	0.0975
93tm5	0.4651	0.2661	0.1826	-0.5920	-0.3901	-0.4206
95tm3	0.4863	0.0055	-0.4094	0.4111	0.3576	-0.5468
95tm4	-0.1434	0.6938	0.5547	0.3810	0.1481	-0.1525
95tm5	0.4614	0.3332	-0.2509	0.3267	-0.4394	0.5598
Eigenvalue	0.2703	0.1159	0.0587	0.0313	0.0228	0.009
% of Variation	53.21%	22.81%	11.56%	6.16%	4.49%	1.77%

TABLE 3B.

PCA [9597] Correlation Matrix

Bands	95tm3	95tm4	95tm5	97tm3	97tm4	97tm5
95tm3	1.0000	-0.2938	0.7648	0.6686	-0.2538	0.5897
95tm4	-0.2938	1.0000	0.0283	-0.2048	0.5866	-0.0318
95tm5	0.7648	0.0283	1.0000	0.5937	0.1313	0.7242
97tm3	0.6686	-0.2048	0.5937	1.0000	-0.3611	0.8261
97tm4	-0.2538	0.5866	-0.1313	-0.3611	1.0000	-0.1791
97tm5	0.5897	-0.0318	0.7242	0.8261	-0.1791	1.0000

PCA[9597] Eigenvector Matrix (from Correlation Matrix)

	Component					
Bands	**1**	**2**	**3**	**4**	**5**	**6**
95tm3	0.4785	0.0283	-0.5807	-0.0207	-0.4939	0.4343
95tm4	-0.1720	0.6939	0.3308	-0.4724	-0.3670	0.1468
95tm5	0.4592	0.2870	-0.3126	-0.4452	0.4276	-0.4775
97tm3	0.4939	0.0290	0.4066	0.3465	-0.4596	-0.5085
97tm4	-0.2432	0.6176	-0.3664	0.6320	0.0827	-0.1380
97tm5	0.4770	0.2304	0.3950	0.2423	0.4695	0.5331
Eigenvalue	0.2566	0.1188	0.0435	0.0313	0.0177	0.0064
% of Variation	54.10%	25.05%	9.17%	6.60%	3.73%	1.35%

Information on the type of change represented by each component can be inferred partly by examination of the algebraic signs on the eigenvectors corresponding to each band at each date (Table 3a and b). For example, no clear pattern existed in eigenvectors between dates for the first and second component of both change images (PCA[9395] and PCA[9597]). These components were deemed to represent overall variation across all pixels in the study area, in agreement with the findings of Byrne *et al*. (1980) and Fung and LeDrew (1987; 1988). A pattern in the eigenvectors was apparent, however, for component 3. In addition, clearing areas were found to be spectrally distinct from surrounding forest in the component 3 images. The differences between bands 3 and 4 in both component 3 images and the relationship of band 3 to 4 in the NDVI indicates a change in "greenness". A pattern was also apparent in component 4 for both change images. The differences between all bands in the component

4 images were reasoned to represent changes in overall "brightness". Patterns of change in eigenvectors were also discovered in components 5 and 6 for each change image. It was concluded however, from evaluation of the corresponding single component imagery, that this variation was likely attributable to factors such as seasonal vegetation variations and soil moisture changes between dates and not forest changes. Components 3 and 4 for both time periods showed the best spatial discontinuity in the change areas of interest and were chosen for thresholding.

Kappa Optimization for Thresholding Change Images

The optimal thresholds for detecting both forest clearing and vegetation regrowth were determined for each two-date NDVI differenced image, and for components 3 and 4 for each time period in the PCA analysis (Table 4). Overall Kappa was considerably higher for component 3 in both time periods (0.72 for 1995-97, and 0.73 for 1993-95) than for component 4 (0.58 and 0.55, respectively). Given the higher Kappa values for clearing and regrowth, component 3 was chosen over component 4 for the PCA change detection classification and subsequent accuracy assessment. The overall Kappa for the NDVI difference image classification of clearing, no change, and regrowth was 0.78 for DIF[9395] and 0.76 for DIF[9597]. These Kappas were higher than the thresholded principal component images at each time period.

TABLE 4.

Clearing Change

Image	DIF[9395]	DIF[9597]	PC3[9597]	PC4[9597]	PC3[9395]	PC4[9395]
Mean	99.7	128.7	49.1	107.8	54.3	70.8
std.dev	18.2	16.9	5.4	5.6	6.3	5.0
Threshold	< 44	< 76	> 121	> 137	< 85	> 118
Clearing Kappa	0.77	0.79	0.69	0.61	0.71	0.59
Regrowth Threshold	> 183	> 163	< 108	< 109	> 124	< 101
Regrowth Kappa	0.77	0.78	0.79	0.57	0.79	0.55
Overall Kappa	0.78	0.75	0.72	0.58	0.73	0.55

Accuracy Assessment and Comparison of Methods

The two-date thresholded images for each method were combined into three-date images (NDVI-DIFF and PCA) to facilitate comparison with the three-date RGB-NDVI classification (Table 5). User's (U) and producer's (P) accuracy were calculated for each of the 7 classes from each method. Overall accuracy, the percentage of pixels classified as "correct" among those sampled, was highest with the RGB-NDVI method (85%) followed by the NDVI-DIFF (82%) and PCA (74%) classifications. Thus, the RGB-NDVI classification resulted in the highest Kappa (0.83), followed by the NDVI-DIFF method (0.79) and PCA method (0.69). The Z-stat was calculated for each matrix and compared to the normal distribution to test if the Kappa of an individual error matrix was significantly different from random. The high Z-stat values for each method indicated that all were significant at the 95% level of confidence. A test statistic (Z) was calculated based on the Kappa (K_i) values and Kappa variance (var(K_i)) of two separate error matrices (i). This value tested for significant difference

between the results of two error matrices (Congalton and Green, 1999). The Z test statistic comparing the NDVI-DIFF and PCA methods (1.89) was slightly less than the critical Z value (1.96) for an alpha of 0.05, thus indicating no significant difference between these methods. There was also no significant difference between the Z test statistic comparing the RGB-NDVI and NDVI-DIFF methods (0.93) and the normal distribution. There was a significant difference between the RGB-NDVI and PCA methods (P< 0.05, Z=2.83).

TABLE 5.

Error Matrix for NDVI-DIFF Method

Reference Data

Classified Data	1	2	3	4	5	6	7	Row Total
1	7	0	0	0	2	0	3	12
2	4	29	1	0	0	0	2	36
3	0	0	21	0	0	0	2	23
4	0	0	0	27	1	0	0	28
5	0	0	0	5	24	0	2	31
6	0	0	1	0	0	24	4	29
7	3	2	1	1	1	2	36	46
Column Total	14	31	24	33	28	26	49	205

Error Matrix for PCA Method

Reference Data

Classified Data	1	2	3	4	5	6	7	Row Total
1	4	1	0	0	3	0	8	16
2	3	25	1	0	1	0	3	33
3	0	4	23	0	0	0	1	28
4	0	0	0	22	2	0	0	24
5	1	0	0	8	22	0	0	31
6	0	0	0	0	0	25	6	31
7	6	1	0	3	0	1	31	42
Column Total	14	31	24	33	28	26	49	205

Error Matrix for RGB-NDVI Method

Reference Data

Classified Data	1	2	3	4	5	6	7	Row Total
1	12	3	0	0	1	0	2	18
2	0	24	0	0	0	0	0	24
3	0	0	24	0	0	0	5	29
4	0	0	0	30	2	0	0	32
5	0	0	0	1	22	0	2	25
6	0	0	0	0	0	24	1	25
7	2	4	0	2	3	2	39	52
Column Total	14	31	24	33	28	26	49	205

		NDVI-DIFF		PCA		RGB-NDVI	
	Forest Change Class	**U†**	**P‡**	**U**	**P**	**U**	**P**
1	cleared before 93 regrowth 95-97	58.3%	50.0%	25.0%	28.6%	66.7%	85.7%
2	cleared before 93 regrowth 93-97	80.6%	93.6%	75.8%	80.7%	100.0%	77.4%
3	cleared before 93 regrowth 93-95, cleared 95-97	91.3%	87.5%	82.1%	95.8%	82.8%	100.0%
4	cleared 93-95 no regrowth	96.4%	81.8%	91.7%	66.7%	93.8%	90.9%
5	cleared 93-95 regrowth 95-97	77.4%	85.7%	71.0%	78.6%	88.0%	78.6%
6	cleared 95-97	82.8%	92.3%	80.7%	96.2%	96.0%	92.3%
7	no change	78.3%	73.5%	73.8%	63.3%	75.0%	79.6%
	Overall Accuracy	82.0%		74.2%		85.4%	
	Kappa	0.79		0.69		0.83	
	Z-stat	24.63*		19.32*		28.05*	

†User's Accuracy; ‡Producer's Accuray;

Test Statistic (Z) for Pairwise Comparison of Two Error Matrices

Matrices	**K1**	**Var(K1)**	**K2**	**Var(K2)**	**Z**
ndvi-diff vs. pc3	0.7857	0.0010	0.6946	0.0013	1.89
ndvi-diff vs. rgb-ndvi	0.7857	0.0010	0.8262	0.0009	0.93
pc3 vs. rgb-ndvi	0.6946	0.0013	0.8262	0.0009	2.83*

*Significant at $\alpha=0.05$ (Zcrit=1.96)

Discussion

The objective of this study was to develop an accurate and efficient change detection method to extract land cover change information from a time-series satellite image database for the Maya Biosphere Reserve (Hayes 1999). The radiometric normalization technique proved easy to perform and practical, especially considering the lack of ancillary information (slope, aspect, sun angle, earth-sun distance, soil conditions, etc.) and *in situ* atmospheric data. The method used to generate reference data from the visual interpretation of TM color composite imagery (Cohen *et al*., 1998) was crucial in determining the appropriate change thresholds and in supporting accuracy assessment procedures, as no other reliable historical reference data was available for this remote and largely inaccessible study area.

The effective use of remote sensing as a tool for generating land cover information is highly dependent on the measurable quality of this information (Congalton and Green, 1999). The assessment of land cover or change detection classification accuracy measures the quality of a classification method, both on its own and in relation to other methods. In this study, the RGB-NDVI method was found to have the highest overall accuracy at 85.4%, which meets the level (85%) that the U.S. Geological Survey has recommended for acceptability of classification results (Anderson *et al.*, 1976).

The accuracy of the RGB-NDVI method was not significantly different from results obtained with the NDVI-DIFF method. These two methods used the same data (NDVI from each date) so it was not surprising that they resulted in similar classifications. The RGB-NDVI method relied on unsupervised classification (three dates at a time) and analyst identification of clusters thus avoiding the difficulties in selecting appropriate thresholds between change and no change values. NDVI image differencing is mathematically simple and easy to interpret, but it still relies on thresholding for change classification. The Kappa maximizing decision rule was preferred over more subjective thresholding decisions. In contrast to thresholding, the grouping of pixel clusters of similar spectral characteristics based on a maximum likelihood criterion in combination with visual image interpretation proved to be a more efficient way to identify areas of clearing and regrowth between dates of imagery.

The RGB-NDVI used a different band subset and a different classification technique than the PCA method, and the results were significantly different. It was interesting to find that both NDVI methods, which used information from TM bands 3 and 4, outperformed the PCA method, which incorporated TM band 5. It is possible, however, that the added information from TM 5 may have been lost by choosing a single PCA change component. Some variation explained by changes of interest may have been located in components 4 and 5, and therefore not included after component 3 was selected for thresholding. Furthermore, the algebraic signs on the eigenvectors can be interpreted in terms of "greenness" and "brightness" changes, but this is subjective and not based on standard correlation, such as that associated with the NDVI. Therefore, the interpretation and thresholding of PCA change imagery can be more complicated than NDVI differencing or RGB-NDVI classification.

In addition to achieving a satisfactory level of accuracy, it was desired that the change detection method could be easily transferable to local government agencies and NGOs working in the region. These NGOs are responsible for updating change detection maps to support conservation-based decision making by local participants. The RGB-NDVI method was considered to be the most effective of change detection methods examined in this study for two primary reasons.

First, the RGB-NDVI method allowed interpretation and classification of forest changes for three dates at a time. The other methods required thresholding change and no change two dates at a time. Analysis of three or more dates allows trends to be examined at more than one interval of time. For example, seven dates of satellite imagery have been acquired and processed thus far in MBR monitoring project (Hayes 1999). Processing three dates at a time, the RGB-NDVI method classified change in three steps while the other methods would need six steps to perform the same classification.

Second, additional information can be interpreted from a three-date RGB-NDVI unsupervised classification than from the thresholding of two-date change images. With thresholding, only clearing, no change, and regrowth can be interpreted between two dates. The naming of RGB-NDVI clusters, based on NDVI values at each date and their variations between dates, can take into account temporal interpretation about the "from" and "to" identifiers of change. For example, the RGB-NDVI method allows delineation of low to high NDVI areas of no change (relative green biomass levels). This information can be important in land use identification when combined in a time series (e.g. the delineation of persistent agriculture or pasture from early regenerating fallowed land, and relatively undisturbed forest).

Conclusions

We have compared three change detection methods (NDVI differencing, PCA change detection, and RGB-NDVI classification) for monitoring time-series change in a tropical moist forest. The objective was to identify the method that most accurately and efficiently extracted forest change information from Landsat TM imagery of the MBR. By validating and comparing these methods, we intended to justify the use of a standard method for the continued study of forest change in the region. The RGB-NDVI method is recommended for its high level of accuracy, its ease in interpretation, and its utility in technology transfer to local NGOs and government agencies for future land cover and land use monitoring.

The accuracy assessment resulted in a measure of the quality of the change information. Such measures are vital when important natural resource decisions are based on satellite-derived information, as is the case with the forest-monitoring program in the MBR. The change detection maps are used to support ecological research and socio-economic studies of the driving forces and environmental consequences of land cover and land use change in the region. Kristensen *et al.* (1997) claimed that the forest change detection mapping of the MBR from satellite imagery was considered the "most powerful monitoring tool" for Conservation International, local government agencies and other NGOs working in the region. The continued monitoring of forest clearing in the MBR (Sader *et al.*, In Press) relies on accurate and efficient techniques, as developed and tested in this study, for extracting quantitative forest change data from remotely sensed images.

Acknowledgements

Literature Cited

Anderson, J.R., E.E. Hardy, J.T. Roach, and R.E. Whitmer, 1976, *A land use and land cover classification system for use with remote sensor data*, Geological Survey Professional Paper 964, U.S. Geological Survey, Washington, D.C., 28p.

Byrne, G.F., P.F. Crapper and K.K. Mayo, 1980, Monitoring land cover change by principal component analysis of multi-temporal Landsat data, *Remote Sensing of Environment*, 10:175-184.

Cohen, W.B., M. Fiorella, G. Gray, E. Helmer and K. Anderson, 1998, An efficient and accurate method for mapping forest clearcuts in the Pacific Northwest using Landsat imagery, *Photogrammetric Engineering and Remote Sensing*, 64:293-300.

Conese, C.G., G. Maracchi, F. Miglietta, F.Maselli, and V.M. Sacco, 1988, Forest classification by principal components analysis of TM data, *International Journal of Remote Sensing*, 9:1597-1612.

Congalton, R.G., 1991, A review of assessing the accuracy of classifications of remotely sensed data, *Remote Sensing of Environment*, 37:35-46.

Congalton, R.G. and K. Green, 1999, *Assessing the Accuracy of Remotely Sensed Data: Principles and Practices*, CRC Press, Boca Raton, Florida, 137p.

Coppin, P.R. and M.E. Bauer, 1996, Digital change detection in forest ecosystems with remotely sensed imagery, *Remote Sensing Reviews*, 13:207-234.

DeGloria, S.D, 1984, Spectral variability of Landsat-4 Thematic Mapper and Multispectral Scanner data for selected crop and forest cover types, *IEEE Transactions on Geoscience and Remote Sensing*, 2:303-311.

Eastman, J.R. and M. Fulk, 1993, Long sequence time series evaluation using standardized principal components, *Photogrammetric Engineering and Remote Sensing*, 59:1307-1312.

Eckhardt, D.W., J.P. Verdin, and G.R. Lyford, 1990, Automated update of an irrigated lands GIS using SPOT HRV imagery, *Photogrammetric Engineering and Remote Sensing*, 56:1515-1522.

ERDAS, 1997, *ERDAS (v.8.3) Field Guide, Fourth edition*, ERDAS, Inc., Atlanta, Georgia, 656p.

Fung, T. and E. LeDrew, 1987, Application of principal components analysis to change Detection, *Photogrammetric Engineering and Remote Sensing*, 53:1649-1658.

Fung, T. and E. LeDrew, 1988, The determination of optimal threshold levels for change detection using various accuracy indices, *Photogrammetric Engineering and Remote Sensing*, 54:1449-1454.

Green, K., D. Lempka and L. Lackey, 1994, Using remote sensing to detect and monitor land-cover and land-use change, *Photogrammetric Engineering and Remote Sensing*, 60:331-337.

Hall, F.G., D.E. Strebel, J.E. Nickeson, and S.J. Goetz, 1991, Radiometric rectification: toward a common radiometric response among multidate, multisensor images, *Remote Sensing of Environment*, 35:11-27.

Hayes, D.J., 1999, Remote sensing for monitoring land cover and land use change in the Maya Biosphere Reserve, Guatemala, Unpublished M.Sc. Thesis, University of Maine, Orono, 194pp.

Horler, D.N.H. and F.J. Ahern, 1986, Forestry information content of Thematic Mapper data, *International Journal of Remote Sensing*, 7:405-428.

Jensen, J.R.,1996, *Introductory Digital Image Processing*, *Second edition*, Prentice-Hall, Upper Saddle River, NJ, 316p.

Jensen, J.R., K. Rutchey, M.S. Koch, and S. Narumalani, 1995, Inland wetland change detection in the Everglades Water Conservation Area 2A using a time series of normalized remotely sensed data, *Photogrammetric Engineering and Remote Sensing*, 61:199-209.

Kristensen, P.J., K. Gould, and J.B. Thomsen, 1997, Approaches to field-based monitoring and evaluation implemented by Conservation International (June 1997) *Proceedings and Papers of the International Workshop on Biodiversity Monitoring, Brazilian Institute for Environment and Renewable Resources*, Pirenopolis, Brazil, pp. 129-144.

Lambin, E.F., 1994, *Modelling Deforestation Processes: A Review*, Tropical Ecosystem Environment Observations by Satellites (TREES) Research Report No.1, European Commission, Luxembourg.

Lillesand, T.M. and R.W. Keifer, 1994, Remote *Sensing and Image Interpretation*, *Third edition*, John Wiley and Sons, New York, 750p.

Lyon, J.G., D. Yuan, R.S. Lunetta, and C.D. Elvidge, 1998, A change detection experiment using vegetation indices, *Photogrammetric Engineering and Remote Sensing,* 64:143-150.

Macleod, R.D. and R.G. Congalton, 1998, A quantitative comparison of change-detection algorithms for monitoring eelgrass from remotely sensed data, *Photogrammetric Engineering and Remote Sensing*, 64:207-216.

Muchoney, D.M. and B.N. Haack, 1994, Change detection for monitoring forest Defoliation, *Photogrammetric Engineering and Remote Sensing,* 60:1243-1251.

Nations, J.D., R.B. Primack, and D. Bray, 1998, Introduction: the Maya Forest, *Timber, Tourists, and Temples*, (Primack, R.B., D. Bray, H.A. Galleti, and I. Ponciano, editors), Island Press, Washington, D.C., 426p.

Rencher, A.C., 1995, *Methods of multivariate analysis*, John Wiley and Sons, New York, 627p.

Rindfuss, R.R. and P.C. Stern. 1998. Linking remote sensing and social science: the need and challenges, *People and Pixels, Linking Remote Sensing and Social Science* (National Research Council), National Academy Press, Washington, D.C., 244p.

Running, S.W., P.L. Peterson, M.A. Spanner and K.B. Teubler, 1986, Remote sensing of coniferous leaf area, *Ecology*, 67:273-276.

Sader, S.A., 1989, Multispectral and seasonal characteristics of northern hardwood and boreal forest types in Maine, *Image Processing 89, University of Nevada-Reno*, ASPRS, Bethesda, MD, pp.109-116.

Sader, S.A. and J.C. Winne, 1992, RGB-NDVI colour composites for visualizing forest change dynamics, *International Journal of Remote Sensing*, 13:3055-3067.

Sader, S.A., C. Reining, T. Sever, and C. Soza, 1997, Human migration and agricultural expansion: a threat to the Maya tropical forests, *Journal of Forestry*, 95:27-32.

Sader, S.A., D.J. Hayes, M. Coan, and C. Soza, In press, Forest change monitoring of a remote biosphere reserve, *International Journal of Remote Sensing*.

Schwartz, N.B., 1998, Time series changes in land use: social science report, phase 1. Submitted to University of Maine, Orono. NASA LCLUC Program, Contract NAG5-6041.

Sellers, P.J., 1985, Canopy reflectance, photosynthesis, and transpiration, *International Journal of Remote Sensing*, 6:1335-1372.

Singh, A., 1986, Change detection in the tropical forest environment of northeastern India using Landsat, *Remote Sensing and Tropical Land Management*, John Wiley and Sons, New York, 365p.

Tucker, C.J., 1979, Red and photographic infrared linear combinations for monitoring Vegetation, *Remote Sensing of the Environment*, 8:127-150.

List of Figures and Color Plates

Figure 1. Location of the study area (Landsat WRS Path 20/Row 48, 1997 TM band 5 shown) in relation to the management units of the Maya Biosphere Reserve, El Petén, Guatemala.

Plate 1. Simplified interpretation of three-date RGB-NDVI color composite imagery (top) according to color additive theory (bottom).

Plate 2. Example of the visual interpretation of Landsat TM RGB 453 color composites for developing reference sample points. Air photos and other ancillary information, where available, can be used for interpreter training. Change classes noted are as follows:
A. Cleared between 93-95, no regrowth
B. Cleared between 93-95, regrowth 95-97
C. Cleared between 95-97
D. No change (high biomass)
E. No change (low biomass)